

N.W. Bressloff, J.B. Moss, P.A. Rubini. "Application of a new weighting set for the discrete transfer radiation model". 3rd European Conference on Industrial Furnaces and Boilers. Lisbon, Portugal, 18-21 April 1995. Eds. Leuckel, Collin, Ward, Reis., INFUB pp.208-215, 1995, ISBN 972-8034-02-4

APPLICATION OF A NEW WEIGHTING SET FOR THE DISCRETE TRANSFER RADIATION MODEL

N. W. Bressloff, J. B. Moss and P. A. Rubini
School of Mechanical Engineering,
Cranfield University, Bedford MK43 0AL, England.

ABSTRACT

The discrete transfer radiation model, DT, represents one of the most popular methods used for the modelling of radiation in furnaces. However, it suffers from the “ray effect” produced by finite division of the solid angle hemisphere. The discretisation process yields a set of weighting coefficients for the radiative intensity along each ray tracing direction. A new method of discretisation, which seeks to mitigate the “ray effect”, is presented and compared with the original method. Comparisons are made against infinite cavity analytical solutions and furnace enclosures containing absorbing-emitting-non-scattering media under different thermal conditions.

INTRODUCTION

Accurate heat transfer prediction in a range of combustion situations - including furnace design and optimisation - demands consideration of radiative effects. Many radiation models now exist and are comprehensively reviewed by Viskanta and Menguc (1987). DT is a hybrid model developed by Lockwood and Shah (1981), containing features of the older zone, flux and Monte Carlo methods, and which offers significant advantages of conceptual simplicity, computational economy and suitability for modelling complex geometries. It is widely used in furnace modelling (cf. Charette et al (1992) and Meng et al (1992)) and in a range of other combustion situations.

Notwithstanding the advantages described above, DT suffers from the “ray effect” whereby incomplete information is received at a point from all other points (Lathrop (1968)). Additionally, this becomes more prominent and problematic when scattering is included (Carvalho et al (1991)). Since it is computationally expensive to minimise the “ray effect” by using a large number of directions along which to solve the radiative transfer equation, RTE, a new method for specifying ray directions has been developed by Bressloff et al (1994). This method aims to mitigate the “ray effect” through a more uniform distribution of rays.

Within DT, repeated solution of the RTE in specific directions yields summations for the radiative flux at solid surfaces, and for the radiative source terms within the domain. Intensity and intensity differences, respectively, are multiplied by a set of weighting coefficients; these coefficients depend on the method of discretising the solid angle hemisphere. Unlike the conventional method, based upon the equal division of the polar and azimuthal angles, the new method produces a more even distribution of ray directions by dividing the solid angle hemisphere into quasi-equal areas.

Analytical solutions (cf. Thynell and Lin (1989) and Crosbie and Schrenker (1984)) for the radiative flux to walls in two-dimensional cavities are used to demonstrate the greater accuracy and stability of the new weighting set across a range of typical ray numbers. Superior performance is then demonstrated in a furnace enclosure from the International Flame Research Foundation, IFRF, trials (cf. Hyde and Truelove (1977)), and in an analytical solved three-dimensional furnace (cf. Selcuk (1985)). The latter test case is

especially challenging since radiative energy source terms are evaluated in the presence of large temperature gradients.

THE DISCRETE TRANSFER METHOD

DT is particularly well-suited to coupled flow and heat transfer calculations in arbitrarily shaped geometries. This is because it is superimposed, without modification, upon the CFD grid, and because boundary conditions are easily incorporated. In particular, ray directions relative to a surface, \vec{r}_{rel} , are specified in terms of Cartesian base vectors, $\hat{e}_1, \hat{e}_2, \hat{e}_3$, which define the surface

$$\vec{r}_{rel} = r_1 \hat{e}_1 + r_2 \hat{e}_2 + r_3 \hat{e}_3 \quad (1)$$

and these directions are transformed to an external reference frame by

$$\vec{r} = \begin{pmatrix} e_{1x} + e_{2x} + e_{3x} \\ e_{1y} + e_{2y} + e_{3y} \\ e_{1z} + e_{2z} + e_{3z} \end{pmatrix} \begin{pmatrix} r_1 \\ r_2 \\ r_3 \end{pmatrix} \quad (2)$$

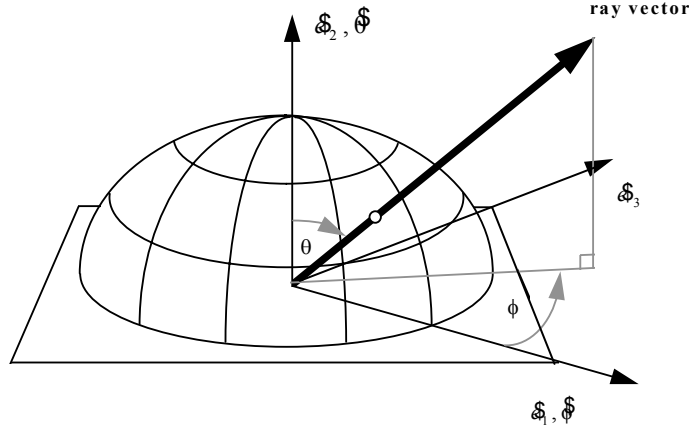


Fig. 1 Conventional discretisation of the solid angle hemisphere

The specification of ray directions in the original weighting set is described in Fig. 1. This alignment of axes yields

$$\vec{r}_{rel} = (\sin \theta \cos \phi, \cos \theta, \sin \theta \sin \phi) \quad (3)$$

and then discrete solid angles are defined by equal divisions of the polar and azimuthal angles θ and ϕ . Each solid angle is represented by a ray located at the centre of the angle and the RTE is solved along all directions for every solid surface element.

The radiative intensity along a single line of sight is evaluated from the integrated form of the radiative transfer equation

$$i_n(s) = \int_0^s i_v(0) \tau_v(0 \rightarrow s) dv + \int_0^s \int_0^s i_{b,v}(s') \frac{\delta \tau_v(s' \rightarrow s)}{\delta s'} ds' dv \quad (4)$$

where τ_v and $i_{b,v}$ are the spectral transmissivity and black body intensity, respectively. The first term in eq. (4) represents radiance at the start of a path that is transmitted to s , and the second term is the sum of energy emitted from intermediate points, s' , that is then transmitted across the remaining path to s . For a grey, homogeneous medium eq. (4) simplifies to a recurrence relation expressing the intensity at the end of a path segment, i_{r-1} , in terms of that at the start of the segment. τ and i are now total properties of the R^{th} cell.

$$i_r = i_{r-1}\tau_R + i_{b,R}(1 - \tau_R) \quad (5)$$

Eq. (5) can be expanded to the origin of the line of sight so as to represent the total path from one solid surface to another

$$i_r = i_0 \prod_{m=1}^M \tau_m^T + \sum_{m=1}^M i_{b,m} \varepsilon_m \prod_{m'=m+1}^M \tau_{m'}^T \quad (6)$$

where ε is the emissivity of the m^{th} cell. Eqs. (5) or (6) are applied twice along each ray direction; away from solid surfaces to calculate energy source terms within the solution domain, and towards surfaces to calculate the incident flux. Since the start value, i_0 , in either direction is unknown, other than for black walls with prescribed temperatures, the process is iterative. i_0 is calculated from the radiative heat flux leaving a surface which, for a grey Lambert surface, is

$$i_0 = \frac{q_+}{\pi} = \frac{1}{\pi} (\sigma T_w^4 - q_-) \quad (7)$$

q_+ and q_- are total outgoing and incident fluxes, respectively, σ is the Stefan-Boltzmann constant and T_w is a solid surface temperature. The incident flux for the n^{th} ray is assumed to be constant for the elemental solid angle, $d\Omega_n$ such that

$$dq_{i,n} = i_{i,n} \cos\theta_n d\Omega_n \quad (8)$$

Hence, integration for this solid angle yields

$$q_{i,n} = i_{i,n} \sin\theta_n \cos\theta_n \sin\Delta\theta_n \Delta\phi_n \quad (9)$$

where θ_n is the angle between the n^{th} ray and the surface normal, and $\Delta\theta_n$ and $\Delta\phi_n$ specify the solid angle polygon. When the radiative recurrence relation is solved across all intersected cells from the hit surface back to the firing surface, the incoming intensity, $i_{i,n}$, is assumed constant within each of the N solid angles, and the total incident flux is

$$q_i = \sum_{n=1}^N i_{i,n} w_n \quad (10)$$

where

$$w_n = \sin\theta_n \cos\theta_n \sin\Delta\theta_n \Delta\phi_n \quad (11)$$

represents the weighting applied to $i_{i,n}$.

Radiative energy source terms in a control volume are calculated from

$$\Delta S_n = \Delta i_n w_n \Delta A \quad (12)$$

and summed for all intersecting rays. It is assumed that each ray occupies a "pencil" equal in area to the projection of the firing surface, and that the "pencil" completely overlaps every control volume that it intersects. These assumptions are justified by Lockwood and Shah (1981) in terms of the expensive cpu penalties that are incurred, for a small improvement in accuracy, when the source terms are calculated according to the proportion of a control volume overlapped by a ray.

This procedure is performed for each surface in turn, q_+ , the radiative flux leaving a surface, is updated using eq. (7) and a convergence criterion is tested based upon the absolute change in the net wall heat flux.

The set of weighting coefficients, w_n , in eq. (10) are functions of ray direction and the solid angles represented by each ray. They also depend on the alignment of the axes (used to discretise the hemispherical solid angle) relative to a solid surface. Hence, the specification of ray directions completely determines a weighting set.

Due to the nature of great circles of the sphere, solid angle polygons closer the polar axis have smaller surface areas. This has the effect that, for constant

$\Delta\theta$ and $\Delta\phi$, weightings are proportional to $\sin 2\theta$ producing a bias towards rays closest to $\theta = \pi/4$. Additionally, rays making a shallow angle to a surface have the same weighting as rays making the same angle with the surface normal. This is in contrast to what is expected from eq. (8) since, if elemental solid angles are equal, the distribution of weightings is given by the cosine function which is single valued for $0 \leq \theta \leq \pi/2$.

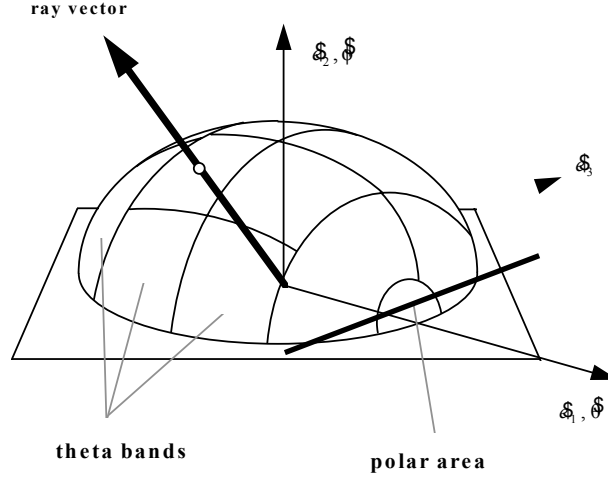


Fig. 2 Quasi-equal area discretisation of the solid angle hemisphere

An important constraint in defining a new weighting set for DT is that cylindrical polar co-ordinates are used. This then maintains the simplicity of the integral calculation for the incident flux using eq. (8). The new weighting set attempts to produce a better representation of the elemental flux equation through a more even distribution of ray directions. The alignment of axes shown in Fig. 2 attempts to achieve this; the polar axis, $\hat{\theta}$, is aligned with a planar base vector, \hat{e}_1 , and the $\hat{\phi}$ axis is aligned with the normal base vector, $\hat{\mathcal{E}}_2$. The ray vector relative to a surface becomes

$$\vec{r}_{rel} = (\cos\theta, \sin\theta\cos\phi, \sin\theta\sin\phi) \quad (13)$$

The hemispherical solid angle is then divided into equal areas - infact, quasi-equal areas are produced due to the requirement of fitting an integer number of areas into individual theta bands. A theta band is defined as the surface area of the hemisphere contained between two values of θ for all values of ϕ . Therefore, each band comprises identical areas, but a slight variation in areas exists between bands. The number of theta bands described throughout the text are in addition to the polar areas. These areas are kept as complete solid angles since a slight improvement in performance is observed when they are not subdivided.

Since, in the original weighting set, the angle between a ray and the surface normal is equal to θ , the direction cosine in eq. (8) is only dependent on θ . For the transformed axes θ is replaced by δ and the direction cosine becomes dependent on both θ and ϕ

$$\cos\delta = \sin\theta\cos\phi \quad (14)$$

Integration of eq. (5) then yields eq. (7) with a weighting set given by

$$w_n = \sin(\Delta\phi_n / 2) \cos\phi_n [\Delta\theta_n - \sin\Delta\theta_n \cos 2\theta_n] \quad (15)$$

COMPARISON OF RESULTS

Few publications address the variation in performance of DT with changing numbers of rays. Shah (1979) has made restricted comparisons and

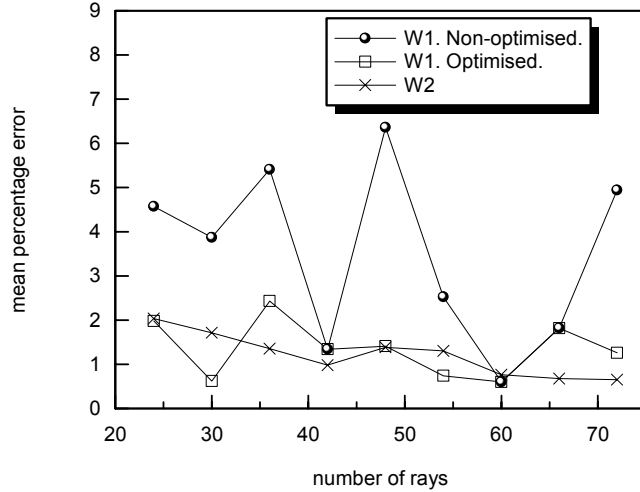
some authors, for example, Carvalho et al (1991) and Fairweather et al (1992), have commented upon flux prediction independence of the number of rays. The variation of wall flux errors with ray numbers in two infinite cavities has been considered recently by Bressloff et al (1994). These results are summarised and reinforced below. The analysis is then extended to two, three-dimensional furnace enclosures. In the discussion that follows, W1 and W2 denote, respectively, the equal polar and azimuthal angle weighting set, and the new, quasi-equal solid angle set.

(a) Radiative flux to a side wall in an isothermal cavity

The first test case comprises a 10 cm square infinite cavity containing an isothermal gas which has a black body intensity of unity and an absorptivity of unity. All the walls are cold ($T_w = 0K$), the side walls have an emissivity of 0.5 and the top and bottom walls have an emissivity of 0.99. This problem specification represents one of the most challenging of the analytical solutions produced by Thynell and Lin (1989) due to the short optical lengths involved, and due to the discontinuities in wall emissivities at the corners.

Fig. 3 Variation of error in flux to a side wall in an isothermal cavity

The mean percentage error of radiative flux to a side wall is calculated by



$$e = \frac{100}{n_g} \sum_2^{N_g+1} \left(\frac{q_{g,a} - q_{g,c}}{q_{g,a}} \right) \quad (16)$$

and is shown in Fig. 3 for a medium range of ray numbers - 24 to 78 rays. $q_{g,a}$ and $q_{g,c}$ denote, respectively, the analytical and computational cell face fluxes summed for the n_g grid cells. Weighting set W2 demonstrates greater accuracy than W1 for most values of ray number, N . More importantly, however, is the superior stability of W2 reflecting the expectation that errors decrease as N increases. This is emphasised by the unsatisfactory performance of the non-optimised solid angle permutations of θ and ϕ for W1. For example, when changing from 3 to 4 theta bands for 48 rays, the mean error increases by up to 5%. Furthermore, since the optimum values of θ and ϕ may vary between different geometries and under different conditions, this produces a high level of uncertainty, and unacceptably large potential errors. In contrast, the number of theta bands for W2 is fixed across a range of ray numbers (cf. Bressloff et al (1994)).

(b) Radiative flux to the top wall in a cavity in radiative equilibrium

Whereas the Thynell and Lin test cases comprise a distributed source of energy, the gas, Crosbie and Schrenker (1984) provide analytical results for a

localised source of energy. A cavity (containing a gas in radiative equilibrium) has three of the four walls at 0K; therefore, the top wall, which has a black body intensity of unity, is the only source of energy. The infinite cavity is 1 metre square and all the walls are black. It is assumed that the gas is purely absorbing with an absorptivity of 0.25. This problem is additionally challenging since there are two discontinuities in the leaving intensities at the corners of the top and side walls.

The heat flux to the bottom wall is the most difficult to calculate accurately due to the fact that it faces the two intensity discontinuities. It is expected, therefore, that this heat flux is very sensitive to the "ray effect".

The temperature field is evaluated from

$$T_{cv} = \frac{\frac{\sigma}{\pi} \sum_{N_{cv}} (1-\tau) w_n \Delta A}{\sum_{N_{cv}} (1-\tau) w_n i_{n,p} \Delta A} \quad (17)$$

whereby all control volume energy source terms have been equated to zero; thus satisfying radiative equilibrium for the gas. N_{cv} is the number of rays crossing a control volume, cv. Fig. 4 demonstrates that large errors exist for weighting set W1 even for 64 rays.

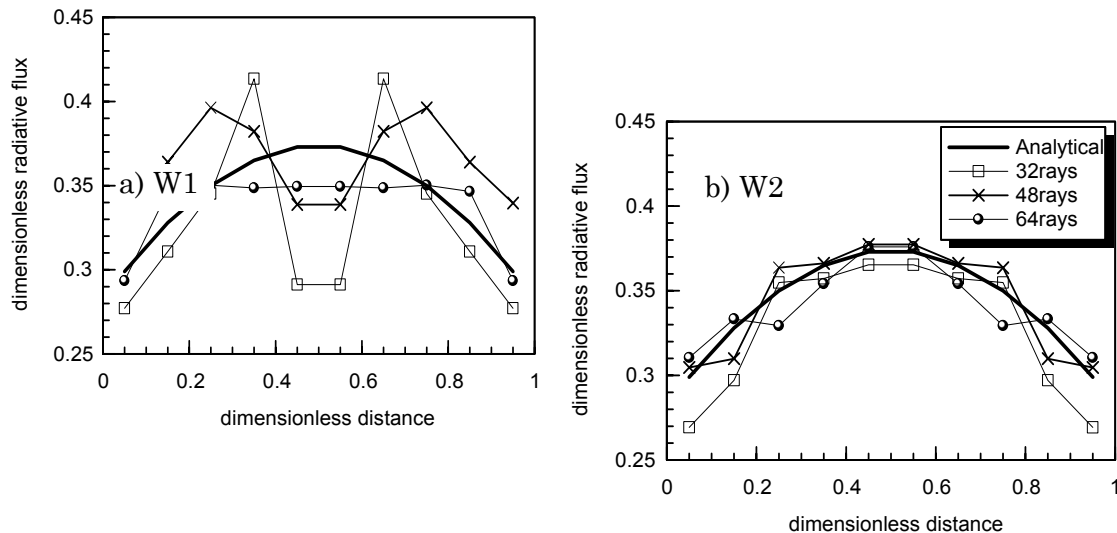


Fig. 4 Comparison between weighting sets for the bottom wall radiative flux of a cavity in radiative equilibrium

(c) Floor and ceiling fluxes in a three-dimensional rectangular furnace

The furnace model described by Hyde and Truelove (1977) is based upon an experimental 3MW natural gas fired furnace of the International Flame Research Foundation, IFRF, M3A (flame 10) trials. This has been regularly used for testing radiation models (cf. Carvalho et al (1991)) comparisons being made against zone model results. Figs. 5a and 5b compare the two weighting sets for the radiative flux to the floor and the roof across a relatively narrow range of ray numbers. The roof flux appears to be more sensitive to changes in ray numbers most probably because it faces the temperature and emissivity discontinuities at the floor corners. The new weighting set exhibits superior performance especially for the flux to the roof. Furthermore, the preferred permutations of θ and ϕ for weighting set W1 are not known a priori.

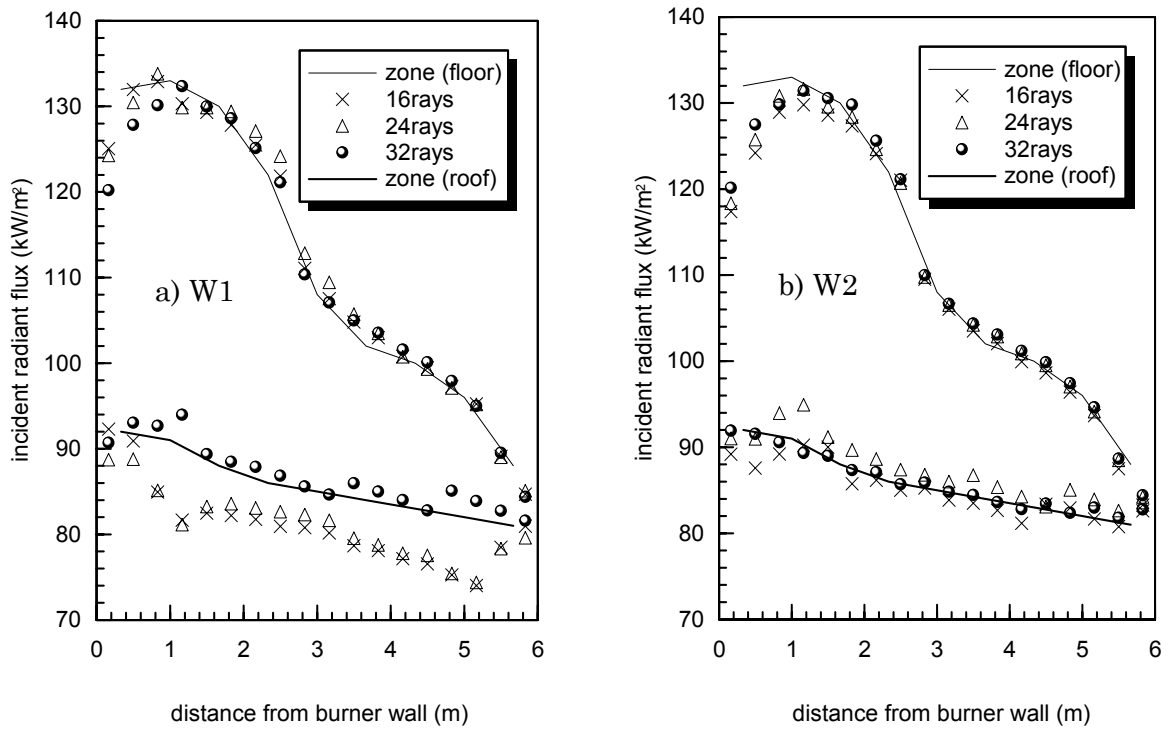


Fig. 5 Comparison between weighting sets for fluxes to the roof and floor in the IFRF furnace M3A trial

(d) Radiative source terms in an analytically solved three-dimensional furnace

Selcuk (1985) presents exact analytical solutions for the distribution of radiative wall fluxes and radiative energy source terms applied to a large-scale experimental tunnel type furnace. Typical of the conditions encountered in industrial furnaces, the temperature field is highly non-uniform; its cross-sectional and axial variation is generated from non-dimensionalised expressions derived from experimental data.

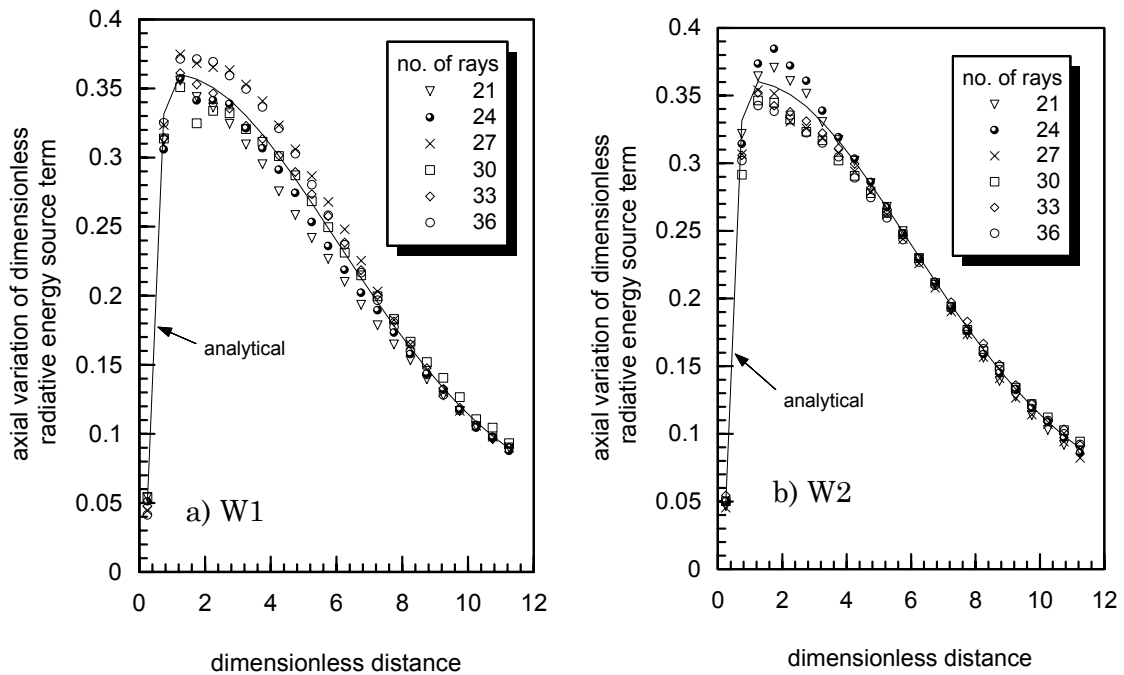


Fig. 6 Comparison between weighting sets for the dimensionless axial source term in an analytically solved furnace (Selcuk (1985))

Fig. 6 shows the dimensionless source term in the medium along nodes closest to the axis calculated for both weighting sets. In accordance with analytical results presented by Selcuk, a 24x2x2 grid has been used in 1/4 of the furnace. The new weighting set, W2, yields greater accuracy than W1 for changing number of rays.

CONCLUSION

A new weighting set has been devised for the discrete transfer radiation model in an attempt to provide a more even distribution of ray directions and, therefore, to lessen the errors produced by the "ray effect". The test cases analysed consistently demonstrate an improvement in performance from the original method of discretisation. Additionally, it has been shown that uncertainty in the selection of ray directions is avoided.

REFERENCES

- Bressloff, N. W., Moss, J.B., Rubini, P.A., A New Weighting Set for the Discrete Transfer Radiation Model, *Cranfield University Report*, sme/nb1/94, 1994.
- Carvalho, M.d.G., Farias, T. and Fontes, P., Predicting Radiative Heat Transfer in Absorbing, Emitting, and Scattering Media Using the Discrete Transfer Method, *Fundamentals of Radiation Heat Transfer ASME*, HTD-Vol. 160, pp.17-26, 1991.
- Charette, A., Haidekker, A., Kocaefe, Y.S., 3-D Comparative Behaviour Of Discrete Transfer And Imaginary Planes Methods For Furnace Modelling, *Canadian Journal of Chemical Engineering* vol. 70 no. 6. pp 1198-1207, 1992.
- Crosbie, A. L. and Schrenker, R. G., Radiative Transfer in Two-Dimensional Rectangular Medium Exposed to Diffuse Reflection, *J. Quant. Spectrosc. Radiat. Transfer* **31**, pp. 339-372, 1984.
- Fairweather, M., Jones, W. P. and Lindstedt, R. P., Predictions of Radiative Transfer from a Turbulent Reacting Jet in a Cross-Wind, *Combustion and Flame*, vol. 89, pp. 45-63, 1992.
- Hyde, D. J. and Truelove, J. S., The Discrete Ordinates Approximation for Multidimensional Radiant Heat Transfer in Furnaces, *AERE R-8502*, AERE Harwell, UK, 1977.
- Lathrop, K. D., Ray Effects in Discrete Ordinates Equations, *Nuclear Sci. and Engineering* **32**, pp. 357-369, 1968.
- Lockwood, F. C. and Shah, N. G., A New Radiation Solution Method for Incorporation in General Combustion Prediction Procedures, *Eighteenth Symposium (International) on Combustion*, pp. 1405-1414, The Combustion Institute, Pittsburgh, 1981.
- Meng, F. L., McKenty, F., Elkaim, D., Camarero, R., Predicting Radiative Heat Transfer In Two-Dimensional Rectangular And Axisymmetric Enclosures Using The Discrete Transfer Method, *Conduction, Radiation and Phase Change Second Int. Conf. Adv. Comput. Method Heat Transfer*, pp 161-180, 1992.
- Selcuk, N., Exact Solutions for Radiative Heat Transfer in Box-Shaped Furnaces, *Journal of Heat Transfer*, vol. 107, pp. 648-655, 1985.
- Shah, N. G., New Method of Computation Of Radiant Heat Transfer in Combustion Chambers, Ph.D. Thesis, Imperial College, London, England, 1979.
- Thynell, S. T. and Lin, W.-Q., Radiation Transfer in Absorbing, Emitting Two-Dimensional Media Bounded by Reflecting Walls, *Nat. Heat Tran. Conf.*, HTD-Vol. 106, Heat Transfer Phenomena in Radiation, Combustion and Fires, pp. 9-16, 1989.
- Viskanta, R. and Menguc, M. P., Radiation Heat Transfer in Combustion Systems, *Prog. Energy Combust. Sci.*, Vol. 13, pp. 97-160, 1987.